The Journal of Experimental Biology 215, 822-832

doi:10.1242/jeb.062505

RESEARCH ARTICLE

Copper and zinc detoxification in *Gammarus pulex* (L.)

Farhan R. Khan*, Nicolas R. Bury and Christer Hogstrand

Nutritional Sciences Division, King's College London, Franklin-Wilkins Building, 150 Stamford Street, London SE1 9NH, UK

*Author for correspondence at present address: Department of Zoology, Natural History Museum, Cromwell Road, London SW7 5BD, UK (f.khan@nhm.ac.uk)

Accepted 18 November 2011

SUMMARY

To negate the toxicity of labile intracellular metals, some aquatic organisms partition metals into specific subcellular locations for detoxification, namely the soluble heat-stable cytosol and insoluble metal-rich granules. The aim of the present study was to characterise these subcellular storage sites in the freshwater crustacean *Gammarus pulex* (Linnaeus) following *in situ* exposures upstream (Drym, low metal) and downstream (Relubbus, elevated metal) of copper- and zinc-rich inflows into the River Hayle (Cornwall, UK). In the cytosol of gammarids exposed at Relubbus, copper and zinc associated to a 7.5-kDa metallothionein-like protein (MTLP) that was largely absent from gammarids prior to exposure. Exposure at Relubbus caused MTLP concentrations to increase 4- to 5-fold between days 2 and 4, indicating an induction response to increased labile intracellular metal. On day 16, spherical calcium-rich granules (0.5–2.5 μmol l^{-1}) were visualised and analysed in the posterior caeca of gammarids exposed at both sites. Following exposure at Relubbus, granules contained trace amounts of copper, but zinc was absent. Granules in gammarids exposed at Drym contained no detectable copper or zinc. Granule formation appeared to be independent of exposure. Within the posterior caeca, granules have been associated with calcium storage during the crustacean molt, rather than in detoxification of trace metals. However, the granular copper burden appeared to follow environmental Cu availabilities. Thus, we describe Cu sequestration within molt-cycle calcium storage granules. As both MTLP concentrations and granule formation in crustaceans are affected upon by molting, we hypothesise that detoxification might impact upon this existing process.

Key words: metal detoxification, metallothionein-like protein, calcium granule, molting

INTRODUCTION

Trace metals accumulate in aquatic invertebrates and are toxic when accumulated more quickly than they can be detoxified and excreted (Rainbow, 2007). Toxicity is caused when labile metal disrupts biological processes – for example, the ionoregulatory disturbance of calcium metabolism by zinc (Hogstrand et al., 1996) or the formation of reactive oxygen species by the changing redox states of copper (Kendrick et al., 1992). To prevent toxicity, free metal can be sequestered, rendering it inert. Subcellular separation of whole organisms or specific tissues has been used to identify five potential locations in which trace metals can reside post accumulation (Wallace et al., 2003). Although metal that accumulates in the cellular debris is often not considered toxicologically relevant (Cain et al., 2004), metals that accumulate in the organelles (including mitochondria and lysosomes) and cytosolic heat-denaturable proteins fractions might induce damage. These subcellular locations have been termed by Wallace as 'metal sensitive fractions' (Wallace et al., 2003). Detoxification occurs in the heat-stable cytosol, in which metals are presumed to bind to thiol groups in the form of the protein metallothionein [MT, or metallothionein-like proteins, MTLPs (Hamer, 1986; Roesijadi, 1996)] and the tripeptide glutathione (Canesi et al., 1998), and within insoluble metal-rich granules (MRGs) (Wallace et al., 2003; Vijver et al., 2004). The operational nature of the subcellular distribution protocol means that metal binding within the fractions is often presumed, but its exact nature is not necessarily determined. This is especially important in those fractions that are presumed to have a role in detoxification. The fate of detoxified metal is more significant when considering trophic availability, with metal bound to MTLP being regarded as bioavailable to predators, whereas metal sequestered to MRGs is generally considered much less trophically available (Wallace and Luoma, 2003; Cheung and Wang, 2005). Differential bioavailability has been shown to lead to differential toxicities, depending on the metal in question. Copper and cadmium bound to an insoluble subcellular fraction comprising MRGs and exoskeleton caused greater localised lipid peroxidation in the gut of zebrafish compared with Cu and Cd bound to the MTLP fraction (Khan et al., 2010a; Khan et al., 2010b). These results were unexpected as it was MTLP-bound metal that was more easily assimilated. Identifying the exact nature of metal binding in these fractions is therefore required.

Cytosolic metal sequestration operates principally through two cysteine-rich peptides – the metal-binding protein MT and the tripeptide glutathione (Hamer, 1986; Canesi et al., 1998). The latter is the most abundant thiol in the cytosol and acts as the first line of defence against metal-induced cytotoxicity. Thus, as intracellular glutathione is bound to metals, the concentration of unbound glutathione decreases. MT has the opposite dose–response relationship to increased intracellular metal compared with glutathione as MT is induced at the transcription level by the presence of increased intracellular metal (Roesijadi, 1996). MTs are cysteine-rich low-molecular-mass cytosolic proteins (typically less than 10 kDa, although MT can exist as a dimer or in polymeric forms) that bind metal ions in clusters of thiolate bonds (–SH). Although MTs from different phyla are not always homologous, they share many characteristics that aid their detection and

quantification. For instance, MTs can be separated from other cytosolic proteins through heat denaturation. Aside from detoxification, MT functions as a chaperone for intracellular trace metal and maintains homeostasis of essential trace metals by regulating metal availability (Hamer, 1986; Roesijadi, 1996; Maret, 2009). However, a positive correlation between MT levels in tissues and environmental metal concentrations has led many authors to view MT as a useful biomonitor of the bioavailabilities of trace metals (Hennig, 1986; Hogstrand and Haux, 1991). More recent studies have shown the increased cycling of MT (i.e. greater turnover), with the increased synthesis and autolysis of proteins, is a plausible response to elevated metal concentrations (Mouneyrac et al., 2002; Ng et al., 2007). In this case, MT concentrations can remain constant during the exposure.

Like MT, it has been suggested that MRGs serve as biomarkers of trace-metal toxicity (Correia et al., 2002), and they are present in most macro-invertebrate phyla (Adams et al., 1997). Three distinct granule types have been described, as follows: type A granules contain calcium but are not homogeneously defined. Calcium phosphate granules containing trace metals are typically associated with detoxification, but granules composed of Ca (and some Mg) in the form of carbonates, sulphates or phosphates are more likely to be temporary Ca stores that often arise during fluxes in Ca concentrations (i.e. during molting) (Meyran et al., 1984); type B granules contain sulphur in conjunction with copper or zinc; and type C granules are more crystalline and are mainly composed of iron, for example in ferritin (Icely and Nott, 1980; Hopkin, 1989; Rainbow et al., 2007). In many macro-invertebrates, and in particular the crustaceans, type A and B granules predominate (Al-Mohanna and Nott, 1987; Al-Mohanna and Nott, 1989). The location of granules, like the composition, has been found to vary, with granules present in the gonad and mantle of the freshwater mussel *Hyridella depressa* (Adams et al., 1997), digestive cells and cuticle of the marine copepod *Tigriopus brevcornis* (Barka, 2007), the cells of the ventral caeca in the amphipod crustacean *Orchestia gammarellus* (Nassiri et al., 2000) and in the marine gammaridean *Gammarus locoppersta* (Correia et al., 2002).

Rather than being separate metal-detoxification strategies, it has been proposed that the formation of type B sulphur-containing granules can occur as a direct result of metallothionein cycling (Rainbow, 2007). As metallothionein enters the lysosome to be broken down as part of its natural cycle, some thiol–metal complexes are degraded within the acidic environment of the lysosome. Lysosomal degradation leads to labile metal (in the case of Cd^{2+} or Zn^{2+} thiol complexes) re-entering the cell to be sequestered again by MT, but, when the thiol–metal bond can withstand degradation (as with Cu^{+}), the intact complex can be concreted with calcium and phosphorus, which are also present in the lysosome. These granules are also known as lysosomal residual bodies or tertiary lysosomes (Luoma and Rainbow, 2008). One species that shows direct evidence of this pathway is the mussel *Mytilus edulis* (George et al., 1982; George, 1983).

In the present study, we investigate the metal binding properties of the heat-stable cytosol and a combined MRG and exoskeleton fraction from *Gammarus pulex* (L.) that were exposed for up to 16 days *in situ* above and below mine drainage shafts (adits) that flow into the River Hayle, Cornwall, UK (Khan et al., 2011). Gammarids exposed below the adit accumulated more copper and zinc, as expected, and, following subcellular fractionation, the heat-stable cytosol and the MRG and exoskeleton (here referred to as 'MRG+exo') fractions combined accounted for no less than 85% of the total metal burden. Over the course of the 16-day exposure, both metals appeared to be redistributed from the heat-stable cytosol to the MRG+exo fraction. By using a number of complimentary techniques, we investigate the nature of metal binding in these two metal-enriched fractions.

MATERIALS AND METHODS

In the present study, the gel chromatography was used to determine the association of cytosolic proteins (MTLPs) with Cu and Zn, and the quantification of the protein was achieved by silver-saturation assays. Metal-rich granules were viewed with a scanning electron microscope (SEM) following cryostat sectioning. The elemental composition of the granules was determined semi-quantitatively by energy-dispersive x-ray microanalysis (EDX). The results from these various techniques are integrated to provide insight into the detoxification processes of *G. pulex*.

Study area and *in situ* exposures

A full description of the *in situ* study conducted in the River Hayle has been published previously (Khan et al., 2011), but salient details are reiterated to describe the exposure of gammarids used in this present study. *G. pulex* were collected from the River Cray (51 deg, 23′, 09.47″ N, 00 deg, 05′, 59.02″ W), in Kent, UK, which has copper and zinc dissolved-water concentrations of 0.81 and 3.62 $\mu g\,l^{-1}$, respectively. Caged subsets (approximately 80–120 individuals) were transplanted to Drym (50 deg, 09′, 23.07″ N, 05 deg, 19′, 54.90″ W) and Relubbus (50 deg, 08′, 23.17″ N, 05 deg, 24′, 32.93″ W) on the River Hayle in Cornwall, UK, for 16 days. Drym is located upstream of the main inflows of copper- and zinc-enriched mine drainage waters, and dissolved-water concentrations are not dramatically different from those of the River Cray (1.3 $\mu g\,Cu\,l^{-1}$ and 7.2 $\mu g\,Zn\,l^{-1}$). Relubbus is downstream of the mine adits and has elevated copper and zinc dissolved-water concentrations of 10.7 and 664.5 $\mu g\,l^{-1}$, respectively. Gammarids were sub-sampled on days 1, 2, 4 and 16 post-exposure and day 0 samples were used for basal measures, as described previously (Khan et al., 2011). A description of the subcellular fractionation protocol used to produce MRG+exo and MTLP fractions has been published previously (Khan et al., 2010a; Wallace et al., 2003). The methodology of Wallace and colleagues (Wallace et al., 2003) produces five operationally defined subcellular fractions; however, the application of this process to organisms with an exoskeleton results in a granular fraction containing both MRGs and exoskeleton (the MRG+exo fraction) (Khan et al., 2010a). To ensure the integrity of the heat-stable cytosol used for detection and quantification of MTLPs, samples were stored at –80°C prior to analysis, and phenylmethylsulfonyl fluoride (PMSF, Sigma-Aldrich, Poole, Dorset, UK) was added at a final concentration of 0.1 $mmol\,l^{-1}$ to prevent protease activity.

Elemental analysis of MTLP and MRG+exo samples

Ca, P, Mg, Fe and S have all been shown to be associated with metal detoxification in metal-rich granules (Hopkin, 1989), whereas S is present in sulfhydryl bonds is the metal-binding ligand on MTLPs within the heat-stable cytosol (Hamer, 1986). These elements, in addition to Cu and Zn, were measured in the MRG+exo and heat-stable cytosol fractions of *G. pulex* exposed at Drym and Relubbus for 0, 4 and 16 days by inductively coupled plasma mass spectrometry (ICP-MS; ELAN 6100DRC, Perkin Elmer, Cambridge, UK). MRG+exo and MTLP fractions were digested in a 1:5 w/v ratio with 60% ultra-pure HNO_3 at 70°C overnight and made up to 3 ml with MilliQ water. For ICP-MS analysis, samples were diluted by a factor or 50. Elemental concentrations in fractions

are expressed as $\mu g\,g^{-1}$ *G. pulex* dry mass (DM). To verify the fraction-digestion procedure, TORT2 lobster hepatopancreas (National Research Council Canada, Ottawa, ON, Canada) and SRM 1566b oyster tissue (National Institute of Standards & Technology, US Department of Commerce, Gaithersburg, MD, USA) were used as standard reference materials. Recoveries of Cu and Zn for both reference materials were consistently within ±10% of the certified concentrations.

Gel chromatography

Heat-stable cytosol samples (20 mg protein in 0.5 ml 10 mmol l^{-1} Tris HCl, operationally defined as containing MTLPs) with the highest (Relubbus exposed, 16 days, N=3) and lowest (0 days, N=3) metal burden were applied to a Sephadex G-75 medium-grade (Amersham Biosciences, Amersham, Buckinghamshire, UK) column (1.6×34 cm) with an optimum separation range of 3–80 kDa. The column was equilibrated with 10 mmol l^{-1} Tris HCl (pH 7.6) and eluted with the same buffer at a flow rate of 1 ml min^{-1} (ÄKTA Prime system pump and fraction collector, Amersham Biosciences) at 6°C. Forty fractions of 3 ml were collected, from which 1 ml was used to measure absorbance at 254 nm and 280 nm (Cecil 3000 Spectrophotometer, Cecil Instruments, Cambridge, UK). Measurement at 280 nm is used for proteins that contain aromatic amino acids, such as tryptophan and tyrosine, whereas 254 nm is more specific to cysteine-rich proteins as it monitors metal thiolate bonds (Morris et al., 1999; Jenny et al., 2004).

To characterise the column, the void volume and total inclusion volume of the column were determined by dextran blue (2000 kDa) and para-nitrophenol (139.11 Da), respectively. Ferritin (450 kDa) was used to confirm the void volume, and bovine serum albumin (BSA, 66 kDa) and cytochrome *c* (12.384 kDa) were used for column calibration (y=–0.21x+1.34; R^2= 0.97). To verify this relationship, rabbit liver MT (Sigma-Aldrich, Poole, UK) was spiked with ^{109}Cd (20 µg MT spiked with 1×10^{-3} MBq ^{109}Cd; GE Healthcare, Chalfont, UK) and was passed through the column. Eluted fractions were monitored for counts per minute (LKB Wallac 1282 CompuGamma, LKB Instruments, Mt Waverly, Vic, Australia), rather than absorbance, and the MT–^{109}Cd product eluted with apparent molecular mass of approximately 10 kDa. The distribution of copper and zinc relative to the eluted fractions of the *G. pulex* heat-stable cytosol was measured by atomic absorption spectrometry [Unicam 929 AA Spectrometer, ATI Unicam, Cambridge, UK, with operational parameters described by Khan and colleagues (Khan et al., 2011)]. The 40 elutions of 3 ml were pooled into 10 samples, each of 12 ml. Pools were concentrated to 0.5 ml through a 3 kDa membrane (Amicon Ultra-15 centrifuge filters, Millipore, Billerica, MA, USA). Concentrates were measured for total protein by protein assay kit (Bio-rad, Hemel Hempstead, UK) based on Bradford's assay (Bradford, 1976). The 0.5 ml concentrates were digested in ultrapure nitric acid (60%,) in a 1:5 w/v ratio at 70°C overnight, evaporated to near dryness and made up to volume with 3% HNO_3. As with ICP-MS, reference materials were used as quality assurance for AAS and were within the certified concentration range. Metal concentrations in the chromatography fractions were expressed as $\mu g\,Me\,mg^{-1}$ protein.

Silver-saturation assay

The silver-saturation assay method (Scheuhammer and Cherian, 1991) was followed to quantify concentrations of the MTLP in *G. pulex* heat-stable cytosol (200 µl per reaction). The principle of the assay is that the binding strength of Ag^+ to the cysteine residues of MT is greater than that of Cu^+ or Zn^{2+} and will displace metals of lesser affinity when MT is bathed in excess Ag^+. The addition of haemoglobin and heating removes Ag^+ from all other ligands except MT. Centrifugation removes the haemoglobin-bound Ag, leaving only Ag^+ exclusively bound to MT. All reagents used were prepared according to Scheuhammer and Cherian (Scheuhammer and Cherian, 1991); 0.5 mol l^{-1} glycine buffer, $AgNO_3$ stock solution (9.27 mmol l^{-1}; 1000 µg Ag^+ ml^{-1}), KCl solution (1.15% w/v), 30 mmol l^{-1} Tris base (pH 8) (TRIZMA Hydrochloride, Sigma-Aldrich) and bovine red blood cell hemolysate made from whole bovine blood (Hemostat Laboratories, Dixon, CA, USA).

Final silver concentrations in the assay product were measured by ICP-MS. Sample preparation for ICP-MS was as follows: 0.75 ml of the final supernatant was digested in an equal volume of concentrated ultrapure HNO_3 (60%) overnight at 70°C. Samples were evaporated to dryness and reconstituted in 5 ml 3% HNO_3. Final samples were diluted 25 fold. To verify the assay, rabbit liver MT and BSA standards at concentrations of 0, 10, 50, 100 and 500 µg ml^{-1} were used as positive and negative controls. BSA caused no increase in the silver concentration of the final supernatant, whereas rabbit liver MT caused silver concentrations to increase linearly between 0 and 100 µg ml^{-1}, after which the concentration did not increase significantly (data not shown). In addition, the MT assay is not interfered with by the presence of other intracellular thiols, such as cysteine or glutathione (Scheuhammer and Cherian, 1991).

The stoichiometry of silver binding to mammalian MT has been defined as 1 µg Ag representing 3.55 µg MT (Scheuhammer and Cherian, 1991). However, invertebrate MTs have been shown to have different binding stoichiometries. Although mammalian MT accommodates seven divalent metal atoms, invertebrate MT might accommodate six (Roesijadi et al., 1991). Additionally, copper, which preferentially binds to thiolate as Cu^+, does not have the same binding stoichiometry as that of divalent ions (Winge, 1991). Without knowing the metal binding stoichiometry of *G. pulex* MTLPs, we could not express concentrations as µg MT g^{-1} tissue (see Scheuhammer and Cherian, 1991) – therefore, it was assumed that the amount of Ag measured in the assay product was proportional to the amount of MTLP (Wu and Chen, 2005). MTLP concentrations are expressed as µg MTLP-bound Ag g^{-1} tissue fresh mass (FM) according to the following equation (Scheuhammer and Cherian, 1991):

$$\mathrm{MTLP} = (C_{\mathrm{Ag}} - C_{\mathrm{Bkg}}) \times V_{\mathrm{T}} \times \mathrm{SDF}/S_V\,, \quad (1)$$

where C_{Ag} is the concentration of silver in the final supernatant (µg Ag); C_{Bkg} is the silver concentration in a 10 mmol l^{-1} HCl-Tris blank sample; V_{T} is the total volume of the assay sample (1.5 ml); SDF is the sample dilution factor, which is based on the mass of tissue and the volume of homogenising buffer. Initial tissue samples were homogenised in a 1:4 w/v ratio (Khan et al., 2011); therefore, the SDF is 4; and S_V is the sample volume used in the assay (0.2 ml).

SEM analysis of microscopic ultrastructures

G. pulex sections were produced by immersion cryofixation with liquid nitrogen, as described by Warley (Warley, 1997). Briefly, individual gammarids were placed along their longitudinal plane in tissue-freezing medium (Triangle Biomedical Sciences, Durham, NC, USA) on a cryostat chuck that was quenched in liquid nitrogen. Following cryofixation, gammarid specimens were sectioned at 20 µm using a Hacker–Bright OTF cryostat (Hacker Instruments, Winnsboro, SC, USA) at a temperature of –20°C. Centre longitudinal sections, in which the entire internal anatomy of the gammarid was visible, were mounted on carbon-covered aluminium

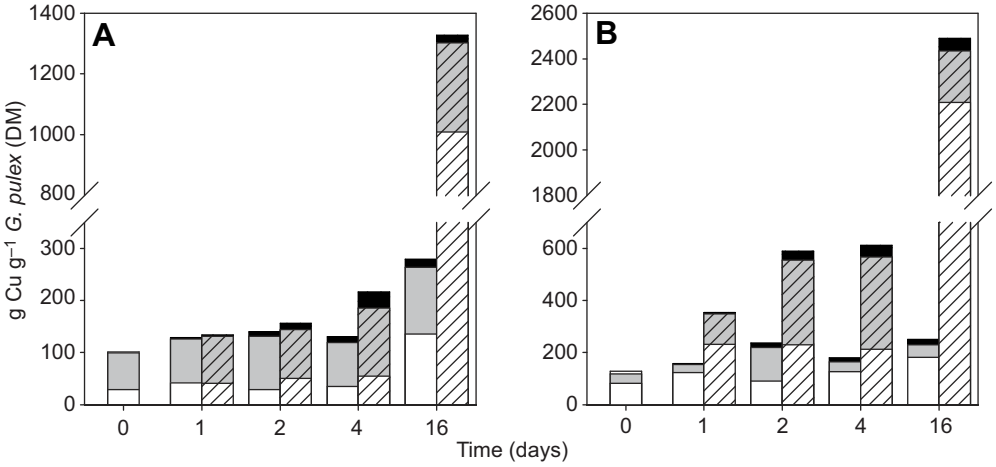

Fig. 1. Subcellular distribution of accumulated (A) Cu and (B) Zn in *G. pulex* exposed at Drym (non-striped bars) and Relubbus (striped bars) over 16 days. Subcellular fractions are shown as MRG+exo (grey bars), MTLP (white bars), and the remaining fractions (cellular debris, organelles and heat-denatured proteins) have been combined as fractions not involved in detoxification (black bars). Each bar represents the data from four replicates (pooled samples). These data are extracted from Fig. 5 (Khan et al., 2011) in which metal concentrations in all subcellular fractions are shown for the entire *in situ* exposure.

stubs for analysis. Sections were visualised by a SEM equipped with a solid-state back-scattered electron detector (FEI, Hillsboro, OR, USA). Where granules were seen, the elemental composition of individual granules was determined semi-quantitatively by EDX. Each EDX spectrum was achieved over an acquisition time of 200 s. In the spectra generated by our analysis, the elemental peaks used were the characteristic Kα emission peaks, that is the peak that corresponds to the x-ray energy emitted when an electron in the L-shell of the element fills a vacancy in the K-shell (the K-shell electron having been ejected, or 'scattered', by the interaction of the SEM incident beam and the specimen). The Kα peak is typically 10-fold greater than the Kβ (generated when the K-shell vacancy is filled by an M-shell electron) and is therefore the more reliable peak for analysis (Warley, 1997). The identity of each peak was assigned automatically by the SEM–EDX software.

For each time-point from which a gammarid was analysed (Relubbus and Drym exposed for 16 days), three individual gammarids were sectioned and multiple sections visualised. Within each section, at least three different granules were analysed by EDX. Individual granules within gammarids exposed at either Relubbus or Drym were similar, and the data presented (Figs 4–6) are representative of our findings. From each individual section, an area of exoskeleton was also analysed. The area of exoskeleton chosen for analysis corresponds to the area of exoskeleton closest to the location of the granules. The carbon pad was also analysed and produced a spectrum that is typical of background continuum radiation.

Wax sectioning and light microscopy

Granules were consistently found in the same location. To relate this to a particular organ within the organism, 10 µm wax sections were made to view the internal biology of *G. pulex*. Standard paraffin wax sectioning, and haematoxylin-and-eosin staining, methodologies were used to produce whole-body cross-sections of *G. pulex* (Agrawal, 1965). Individual gammarids underwent the following steps to produce wax sections: fixation (10% formaldehyde, 90% phosphate-buffered saline for 24 h); washing in 0.9% NaCl; dehydration in an ethanol series (70%, 24 h; 100%, 1 h; 100%, 2 h); clearing (100% chloroform for 2 h); impregnation (paraffin wax at 56°C for 2 h) and embedding (molten paraffin wax for 2 h). Ten-micron sections were produced, and every tenth section was collected. Haematoxylin-and-eosin staining was accomplished by immersing sections in the following solutions: xylene (10 min), ethanol (100%, 3 min; 70%, 3 min), deionised water (30 s), haemotoxylin (5 min), water, 1% HCl (1 min), running tap water, eosin (3 min), 70% ethanol (3 min), 100% ethanol (3 min) and finally xylene (10 min). Sections were viewed through an Olympus S2X12 light-dissection microscope equipped with an Olympus TVO 5XC-2 camera (Olympus Microscopy, Southend-on-Sea, UK)

Statistical analysis

The concentrations of Cu and Zn in the MTLP and MRG+exo fractions of exposed gammarids have been published previously (Khan et al., 2011). By measuring elements associated with metal binding in those fractions, we were primarily concerned with the relationship of Ca, P, Mg, Fe and S to increasing Cu and Zn burdens rather than with their absolute concentrations. Thus, significant relationships were identified by Pearson's correlation. Significant differences in MTLP concentration, as measured by silver-saturation assay, were identified by one-way ANOVA with post-Tukey's honest significant difference (HSD). Statistical analyses were performed using SPSS v.15.0 (SPSS, Somers, NY, USA).

RESULTS

Elemental composition of granular and cytosolic fractions

The total Cu [concentration range: 22.0–1114.9 µg Cu g^{-1} *G. pulex* (DM)] and Zn [66.9–2971.0 µg Zn g^{-1} *G. pulex* (DM)] concentrations in the MRG+exo fraction increased following exposure at Relubbus over 16 days, whereas individuals exposed at Drym (above the adit) remained relatively stable (Fig. 1). As the focus of this work is to characterise metal binding within the MTLP and MRG+exo fractions – the subcellular fractions that were most enriched following exposure – metal burdens in the remaining fractions (cellular debris, organelles, heat-denatured proteins) have been combined in Fig. 1, but are fully described by Khan et al. (Khan et al., 2011). Following subcellular distribution, the percentage recoveries for Cu and Zn in comparison with whole-body burdens were 91.3±18.7% (range 76.1–129.6%) and 86.0±26.1% (range 68.2–139.2%), respectively, as reported by Khan and colleagues (Khan et al., 2011).

Of the elements measured in selected MTLP and MRG+exo fractions to determine any potential role in detoxification, Ca was the most abundant element in the MRG+exo fraction [13366.1–24857.0 µg Ca g^{-1} *G. pulex* (DM)], but it did not increase with increasing Cu and Zn concentrations (Table 1). Although some types of MRGs are calcium rich, the presence of Ca in the exoskeleton within the MRG+exo fraction meant that it was impossible to distinguish exoskeletal Ca from granular Ca using ICP-MS. Mg [164.8–299.8 µg Mg g^{-1} *G. pulex* (DM)] and Fe [34.6–81.4 µg Fe g^{-1} *G. pulex* (DM)] concentrations in the MRG+exo did not correlate with increasing Cu and Zn.

Table 1. Correlation (R^2) of Ca, P, Fe, Mg and S with Cu and Zn concentrations [μg g^{-1} *G. pulex* (DM)] in the MRG+exo and MTLP fractions of *G. pulex* exposed *in situ* at Relubbus or Drym over a 16 day period

		Cu		Zn	
Subcellular fraction	Element	R^2	Equation	R^2	Equation
MRG+exo	Ca	0.20	y=0.064x–1090.6	0.18	y=0.14x–2363.7
	P	0.31*	y=1.74x–1578.8	0.34*	y=4.18x–3846.2
	Mg	0.20	y=4.65x–832.6	0.16	y=9.80x–1715.3
	Fe	0.02	y=3.59x+54.0	0.00	y=3.34x+390.6
	S	0.41*	y=3.01x–1006.7	0.35*	y=6.64x–2138.9
MTLP	S	0.06	y=–0.28x+222.6	0.02	y=0.22x+67.4
	S#	0.52**	y=0.47x+68.2	0.11	y=0.37x+80.13

Gammarids were sampled on days 0, 4 and 16 (three replicates per time and site). In total, 15 data-points were used in each correlation. S in the MTLP was correlated as both μg g^{-1} *G. pulex* (fw) and as μg g^{-1} protein in the MTLP fraction. The latter is indicated by #. Significant Pearson's correlations are denoted by *(P<0.05) and **(P<0.01). Equations (in the form y=mx+c) are shown to characterise the nature of the relationship between the measured elements (x) and Cu or Zn (y), where m is the slope and c is the y-intercept.

P [836.4–1370.9 μg P g^{-1} *G. pulex* (DM)] and S [246.5–566.2 μg S g^{-1} *G. pulex* (DM)] did significantly correlate with increasing Cu and Zn concentrations in the MRG+exo fraction (P<0.05; Table 1). Within the heat-stable cytosol, the ranges of Cu and Zn concentrations during the exposure period were 32.7–308.1 and 16.7–355.5 μg g^{-1} *G. pulex* (DM), respectively. S [63.4–536.9 μg S g^{-1} protein (DM)] correlated with increasing Cu when expressed in terms of protein concentration (P<0.01; Table 1), but not when expressed as tissue weight. S in the MTLP fraction did not correlate with Zn concentrations.

Characterisation of the heat-stable cytosol

Gel filtration

The heat-stable cytosolic samples with the greatest Cu [273.3±37.0 μg Cu g^{-1} *G. pulex* (DM)] and Zn [228.2±44.7 μg Zn g^{-1} *G. pulex* (DM)] concentrations were from those gammarids exposed at Relubbus for 16 days. The typical elution profile of these cytosolic samples (N=3) showed a peak with an elution volume of 63 ml, with the maximum peak height reached at 72 ml (Fig. 2B). Through the calibration of the column, the apparent mass of this protein was calculated to be 7.5 kDa. The maximum peak had an absorbance value of 1.2 at 254 nm and 0.8 at 280 nm (A_{254}/A_{280} ratio of 1.5), suggestive of an amino acid composition that is rich in cysteine (Morris et al., 1999; Jenny et al., 2004). Both Cu and Zn were shown to elute with the 7.5 kDa MTLP. Some Cu and Zn were also associated with a high-molecular weight (HMW) peak that eluted at 33 ml. Accurate size estimations of this peak are difficult because it eluted close to the void volume; however, it could be suggested that the molecular mass is within range of the upper limit of optimum separation (i.e. 80 kDa). Proteins within the HMW range were found to have an A_{254}/A_{280} ratio of approximately 1 (i.e. approximately equal absorbance values at 254 nm and 280 nm). Thus, the HMW proteins are different in molecular mass and amino acid composition to the MTLP.

When the cytosolic elution profile of gammarids with the highest metal burden (Fig. 2B) was compared with the elution profile of heat-stable cytosol with the lowest metal burden [prior to exposure (0 days); Fig. 2A] both the 7.5 kDa MTLP and HMW protein peaks were present. The HMW peak was similar in protein concentration and metal load, but the 7.5 kDa MTLP had much lower absorbances at both 254 nm and 280 nm, although the A_{254}/A_{280} ratio remained similar. The increase in intracellular Cu and Zn concentrations as experienced by those gammarids exposed at elevated environmental concentrations would appear to be associated with the 7.5 kDa protein in the heat-stable cytosol.

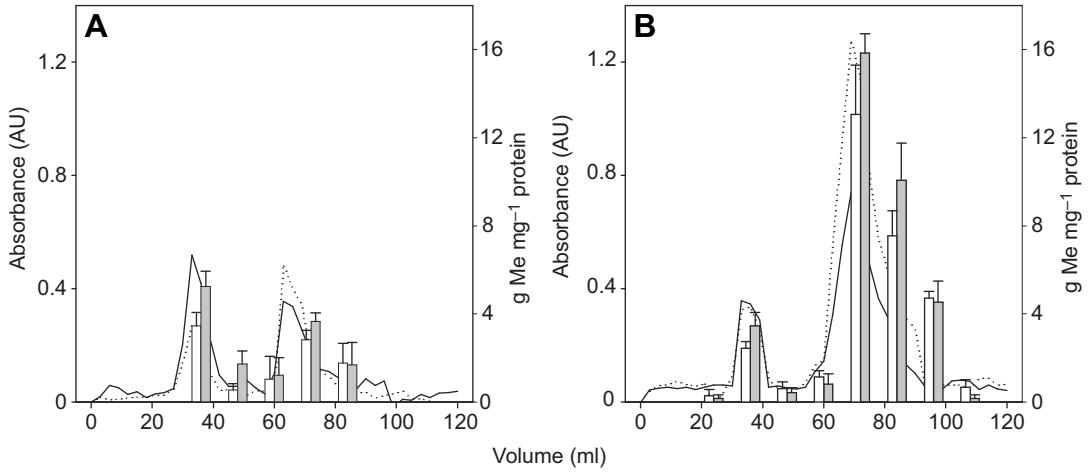

Fig. 2. Size-exclusion chromatograms of *G. pulex* cytosol with (A) lowest and (B) highest Cu and Zn concentrations. Absorbance (in absorbance units, AU) is shown at 254 nm (dotted line) and 280 nm (solid line), with concentrations of Cu (white bar) and Zn (grey bar) expressed in μg metal (Me) g^{-1} protein (means±s.d., N=3 for all measurements). *G. pulex* with the lowest cytosolic Cu and Zn concentrations were individuals sampled prior to exposure (A), and *G. pulex* with the highest cytosolic concentrations were sampled following 16 days exposure at Relubbus (B). Elution profiles show a marked increase of a MTLP with an elution volume of 63 ml (characterised as a 7.5 kDa protein) that elutes with both Cu and Zn.

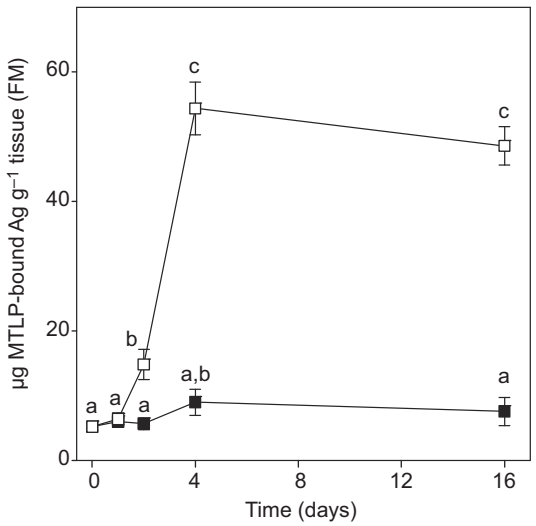

Fig. 3. MTLP concentrations in the cytosol of *G. pulex* exposed at Drym (low Cu and Zn, black squares) and Relubbus (high Cu and Zn, open squares) for 16 days. Concentrations of MTLP are presented as µg MTLP bound to Ag following Ag-saturation assay and then normalised to initial homogenate mass (FM). Mean values (N=3) are shown, with error bars representing 1 s.d. Homologous subsets are indicated by the same letters (P<0.05, two-way ANOVA with *post hoc* Tukey's HSD).

Silver-saturation assay

The basal MTLP concentration was 5.3±0.62 µg MTLP-bound Ag g^{-1} tissue (FM). In the cytosol of gammarids exposed at Drym (above the inflows of metal-enriched water), MTLP concentrations remained close to this basal level, although at day 4 there was a significant increase to 9.0±2.0 µg MTLP-bound Ag g^{-1} tissue (FM) (P<0.05, one-way ANOVA; Fig. 3). At Relubbus, where Cu and Zn concentrations are elevated, MTLP concentrations rose significantly from the basal level to 14.8±2.3 µg MTLP-bound Ag g^{-1} tissue (FM) after 2 days exposure (P<0.05, one-way ANOVA). MTLP concentrations increased further by day 4 to 54.4±4.0 µg MTLP-bound Ag g^{-1} tissue (FM) and remained relatively high at 16 days. Between days 2 and 4 there was a 4–5-fold increase in MTLP concentration in gammarids exposed at Relubbus, which is consistent with the induction of MTLPs in response to exposure to trace metals.

Analysis of granules

Morphology and composition

Granules were visualised in *G. pulex* exposed at Relubbus for 16 days (Fig. 4). This exposure had resulted in the greatest Cu and Zn body burden and the highest metal content within the MRG+exo fraction (Khan et al., 2011). Clusters of spherical granules ranging from 0.5 µm to 2.5 µm in diameter were located dorsally between the exoskeleton and the digestive tract (Fig. 4). Ca, P and O were the most abundant elements, with Ca and P of similar ratio and O more abundant (Fig. 3A,B). Among the other peaks, S was noticeably present. Mg was present at a similar proportion to Na, K and Cl – these are not believed to be important constituents of the mineralised granule and instead are thought to originate from cellular or tissue material that surrounds the granules. Fe was not present within the granules. EDX analysis revealed a detectable Cu load in the granules at 8 KeV, but Zn was absent. This trace amount of Cu was above background levels, as shown by the analysis of the background stub (Fig. 5A). Exoskeleton, which was prominent within the MRG+exo fraction, was also analysed (Fig. 5B,C, showing SEM and EDX for the outermost exoskeleton). The characteristic markings on the exoskeleton are formed by the openings of pore canals, which are used to transport secretions, including Ca, to the surface (Schmitz, 1992). Elemental analysis showed that the exoskeleton was Ca rich, with other elements being present in only trace amounts. Cu and Zn were not found on this outermost layer of exoskeleton, but the detection limit for EDX is in the low parts-per-thousand range and therefore metal could be present at levels below this detection limit.

Gammarids exposed at Drym contained clusters of granules (0.5–2.5 µm, Fig. 6A,B) of a size similar to those that had been found in the Rellubus-exposed individuals (Fig. 4). Following exposure at both sites, granules were consistently located in a similar position, anatomically, and were compositionally similar, containing comparable ratios of Ca, P and O. However, in granules analysed from gammarids exposed at Drym, no peak was detected for Cu, and again Zn was absent (Fig. 6C,D). The presence of granules in Drym-exposed (low Cu and Zn) gammarids is somewhat surprising and would suggest that the formation of granules could be independent of detoxification.

Granule location

In gammarids exposed both above and below the inflow of metal-enriched waters, granular concretions were consistently located dorsally between the exoskeleton and the digestive tract. The relevant anatomy of a gammaridian amphipod (Schmitz, 1992) has been applied to a freeze-dried cross-section of *G. pulex* (Fig. 7A). The cross-section shows three regions of the digestive tract running through the gammarid, namely, the midgut (mg), digestive caeca (dgc, also known as the ventral caeca) and the hindgut (hg). The ventral caeca, often termed the hepatopancreatic caeca in amphipods (Icely and Nott, 1980), has been shown to be the location of metal-sequestering calcospherite granules that increase in number and metal load in response to increased environmental metal concentrations and increased whole-body metal concentrations (Icely and Nott, 1980; Nassiri et al., 2000; Correia et al., 2002).

However, the granules located in the SEM did not appear to be located in areas consistent with the ventral caeca. Two stained masses show the heart and the posterior caeca (Fig. 7D,E, respectively) positioned proximally to the exoskeleton. Granules in all analysed SEM sections appeared to be located within a region that was consistent with the position of the posterior caeca. The posterior caeca are a pair of looped structures that arise from the midgut. They are two of the seven caeca that are found in gammarideans, all of which branch from the midgut – the dorsal caecum, two pairs of ventral caeca and the two posterior caeca (Agrawal, 1965; Schmitz, 1992). Spherical calcium-containing granules have been located within the amphipod posterior caeca, but they have been implicated as functioning as temporary calcium stores within the molt cycle rather than metal detoxification (Graf and Meyran, 1983; Graf and Meyran, 1985).

DISCUSSION

Our initial exposure study showed that *G. pulex* exposed to elevated environmental copper and zinc concentrations partitioned metals to the heat-stable cytosol and a combined MRG+exo fraction, both of which are indicative of detoxification, thereby negating metal-induced toxicity (Khan et al., 2011). In this paper, our aim was to investigate further the metal binding properties of these two fractions. In the heat-stable cytosol, operationally defined as

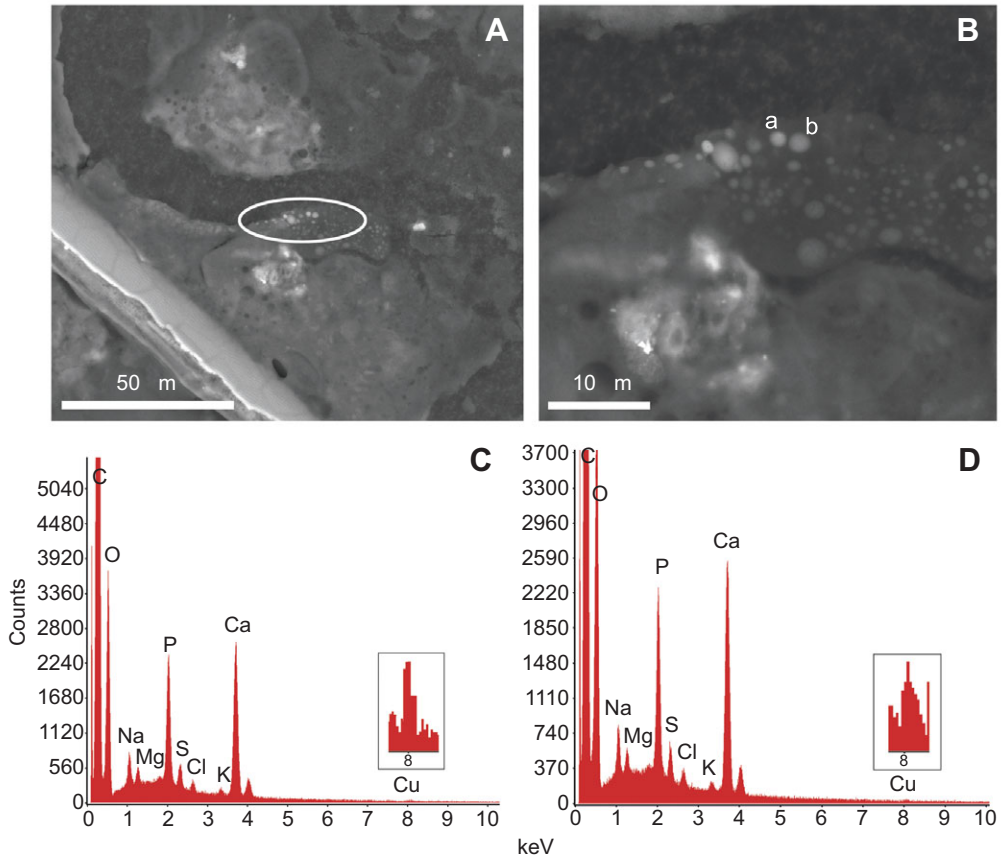

Fig. 4. Electron-dense granules found in *G. pulex* exposed at Relubbus for 16 days shown at magnifications of (A) ×2000 and (B) ×6000. (C,D) Energy-dispersive x-ray microanalysis (EDX) of granules marked 'a' (C) and 'b' (D) reveal that granules contain Ca, P and O as constituent minerals. Detectable quantities of Cu are present in granules (inset magnified on the EDX analysis), but Zn could not be detected.

containing MTLPs, both Cu and Zn were specifically associated to a 7.5 kDa protein that had a high ratio of cysteine residues. Having previously used a subcellular fractionation procedure to distinguish the different pools of accumulated metal, we encountered difficulty in separating metal bound to granules and exoskeleton as a combined MRG+exo pellet was produced. When analysed separately by SEM, the outermost exoskeleton [i.e. the Ca-stiffened cuticle (Schmitz et al., 1992)] contained no detectable metal burden, but calcium-containing granules were located in an area corresponding to the posterior caeca and were shown to incorporate Cu, but not Zn.

The 7.5 kDa protein that eluted with Cu and Zn appears to be a MTLP and shared a number of common features with MTs – it was heat stable, of low molecular mass, cysteine rich (A_{254}/A_{280} ratio ~1.5) and had an increased presence in the cytosol following exposure at elevated environmental concentrations. Kojima and colleagues (Kojima et al., 1991) listed these characteristics, among others that are used to identify proteins conclusively as MT, but, without the amino acid sequence, we are unable to demonstrate homology to other MTs. Thus, the *G. pulex* cytosolic protein is described as a MT-like protein. Comparing the gel-filtration chromatography elution profiles with those of other studies that have also used a Sephadex G-75 column to isolate MTLPs (Mounaji et al., 2002; Wu and Chen, 2005), the chromatograms produced by *G. pulex* heat-stable cytosol showed remarkable similarities with those of metals eluting with an MTLP of less than 10 kDa. A key property of MT is that it is induced by exposure to trace metals (Hamer, 1986; Roesijadi, 1996). This was demonstrated with the silver-saturation assay in which gammarids exposed at Relubbus increased their overall MTLP concentration, particularly between days 2 and 4 (Fig. 3), which would be consistent with the synthesis of new proteins (i.e. induction) rather than the turnover of existing proteins (i.e. breakdown followed by synthesis). However, the greatest increase in cytosolic Cu and Zn concentrations was between days 4 and 16 (Fig. 1), which suggests an apparent misalignment of dose and response. In gammarids exposed at Relubbus, the increase in Cu and Zn concentrations in the MTLP fraction in the acute phase of the exposure (i.e. 0–4 days) was accompanied by a 4–5-fold increase in MT concentration. This would seem to be a disproportionate response, but the MTLP response might not be proportional to the metal concentration (i.e. not a 1:1 ratio as we have presented here in the absence of *Gammarus* MT binding stoichiometry). Scheuhammer and Cherian (Scheuhammer and Cherian, 1991) calculated a 1 µg Ag to 3.55 µg MT ratio, and therefore a slight increase in labile intracellular metal might cause the increase of MTLP levels that we present. As metal concentrations in the heat-stable cytosol largely increased between days 4 and 16, there was no further increase in MTLP levels. Colvin and colleagues (Colvin et al., 2010) suggested that, with Zn at least, MT might be involved in buffering and muffling reactions that are caused by the Zn^{2+} binding to MT with differing affinities. From this, we could postulate that, at day 4, MTLPs had been induced following exposure, but the MTLPs were not saturated. At day 16, although intracellular metal concentrations had increased, there was no need for further MTLP induction as existing unsaturated MT could sequester the increased cytosolic metal.

Increased intracellular metal causes the induction of MTLPs at the transcription level, but this often results in a lag phase prior to MT performing the detoxification function (Fig. 3) (Roesijadi, 1996). During this time, glutathione sequesters labile metal and prevents cytotoxicity (Singhal et al., 1987; Elia et al., 2008; Elia et al., 2010). In our study, the involvement of glutathione was not evident, but there are several reasons for this. First, the time-sequence

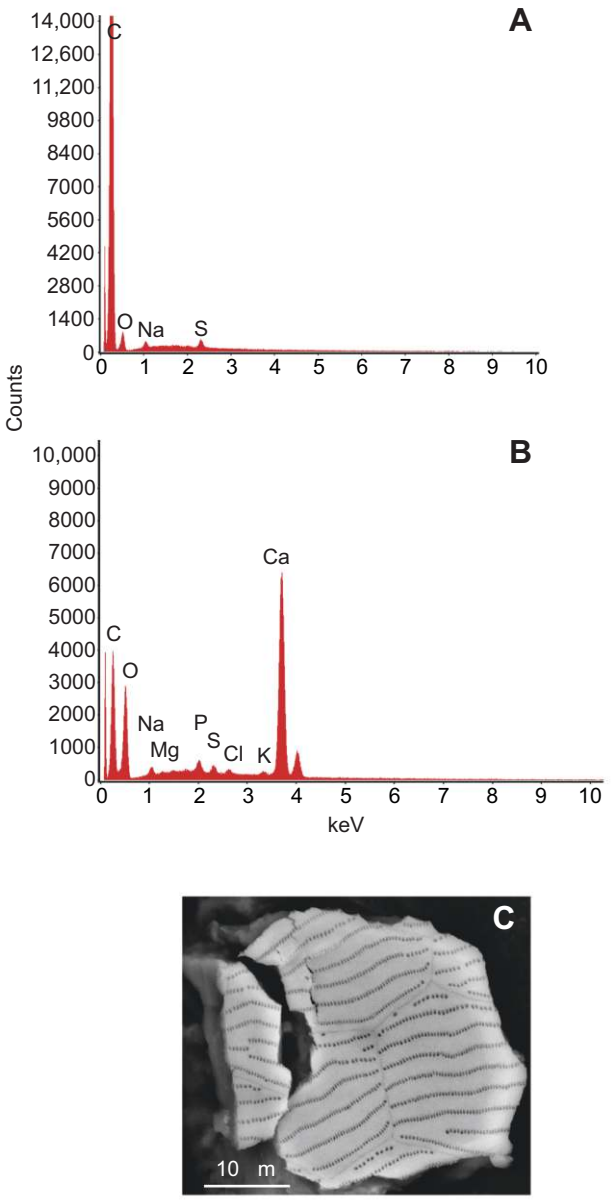

Fig. 5. Energy-dispersive x-ray (EDX) microanalysis spectra of (A) background carbon stub and (B) *G. pulex* exoskeleton. (C) Analysis of the exoskeleton fragment, shown at ×6000 magnification, revealed that was primarily composed of Ca and had no detectable traces of Cu or Zn.

of the glutathione response – glutathione is depleted as it sequesters metal as opposed to MT, which is induced to bind metal. In the present study, the influence of glutathione in the acute phase of the exposure would have been overlooked by our focus on MTLP behavior at days 2, 4 and 16. Second, the tripeptide glutathione ($C_{10}H_{17}N_3O_6S$, molecular mass=0.307 kDa) was below the optimum separation range of the column elution profiles (Fig. 2) and, finally, the silver-saturation assay (Fig. 3) is unaffected in the presence of 40 μmol l^{-1} cysteine or glutathione (Schuehammer and Cherian, 1991). Although it is entirely likely that glutathione was involved in preventing Cu- and Zn-induced cytotoxicity following the exposure of *G. pulex* at Relubbus, it is also likely that, given the parameters of our analysis, the involvement of glutathione was not observed.

Sulphur concentrations in the MTLP and MRG+exo fraction correlated with increases in Cu concentration. In *Orchestia gammarellus* (another amphipod), sulphur and phosphorus in granules correlated with Cu and Zn concentrations (Nassiri et al., 2000). It has been proposed that the sulphur within granules is the same sulphur in thiol groups in MTLPs, with the lysosomal degradation of MTLPs resulting in MRGs, specifically type B granules. This could only occur with metal–thiolate complexes that can withstand reduction in the lysosome, such as Cu-thiolate, which then polymerise to include Ca and P, also present in the lysosome. This lysosomal breakdown of Cu–MT gives rise to the sulphur-containing calcium granules, but the affinity of Zn and thiolate is weaker, and, therefore, following the degradation of Zn-thiolate, Zn is often returned to the cytosol or can be stored within the lysosome as zinc phosphate (Nassiri et al., 2000). In our study, cytosolic sulphur did not correlate with increasing Zn. Thus, Cu alone might have caused the increase in total MT as determined by the silver-saturation assay, and intracellular Zn might have been regulated by MT turnover. This is plausible because Cu-thiolate complexes would be granulised, resulting in the copper and sulphur burden observed in the granules, meaning that new MT would be synthesised to detoxify intracellular copper, but Zn was absent in granules, which would probably mean that Zn-thiolate complexes, once degraded, would separately return to cytosol. The inability to locate zinc-containing granules in this study does not preclude their existence. The concentration of Zn in the MRG+exo fraction would indicate some insoluble storage of Zn in *G. pulex*. Barka (Barka, 2007) found zinc and copper in separate granules in the marine copepod *Tigropus brevicornis*, demonstrating that they do not colocalize within granules.

Calcospherite granules have been recognised for metal storage in numerous crustacean species and are associated with the digestive system within the digestive (ventral) caeca, also termed the hepatopancreatic caeca (Schultz, 1976; Icely and Nott, 1980; Nassiri et al., 2000). Ventral caeca granules are often excreted, and, in this way, the organism is able to reduce the total metal load. The granules found within *G. pulex* were atypical with regard to location and exposure condition. First, the granules were located in the posterior caeca not the digestive caeca, and thus excretion would not necessarily have been their eventual fate. Second, the granules analysed in gammarids exposed at both Drym and Relubbus were compositionally similar in terms of Ca, P, O and S, but differed markedly in copper load. This suggests that the formation and abundance of granules were independent of environmental concentrations of trace metals. Calcium-containing granules have been located within the posterior caeca and are related to the crustacean molt cycle (Graf and Meyran, 1983; Graf and Meyran, 1985; Meyran et al., 1986). Again, that we only located these granules in the posterior caeca does not preclude the existence of other metal-binding granules (i.e. in the digestive caeca) – only that they were not located using SEM in backscatter mode. If type B granules were present as lysosomal residual bodies then they might not have been sufficiently electron dense to be visualised. The copper content of the posterior caeca granules appears not to account for all the copper measured in the MRG+exo fraction.

During the crustacean molt cycle, the posterior caeca are modified in relation to calcium metabolism. Calcium from the old cuticle is reabsorbed into the lumen of the posterior caeca, and the calcium is stored as spherical granules. Over the course of the molt and, in particular, the pre-exuvial period, the posterior caeca lumen is filled with the calcospherite concretions (Graf and Meyran, 1983; Graf and Meyran 1985; Meyran and Graf, 1985). Given the location of

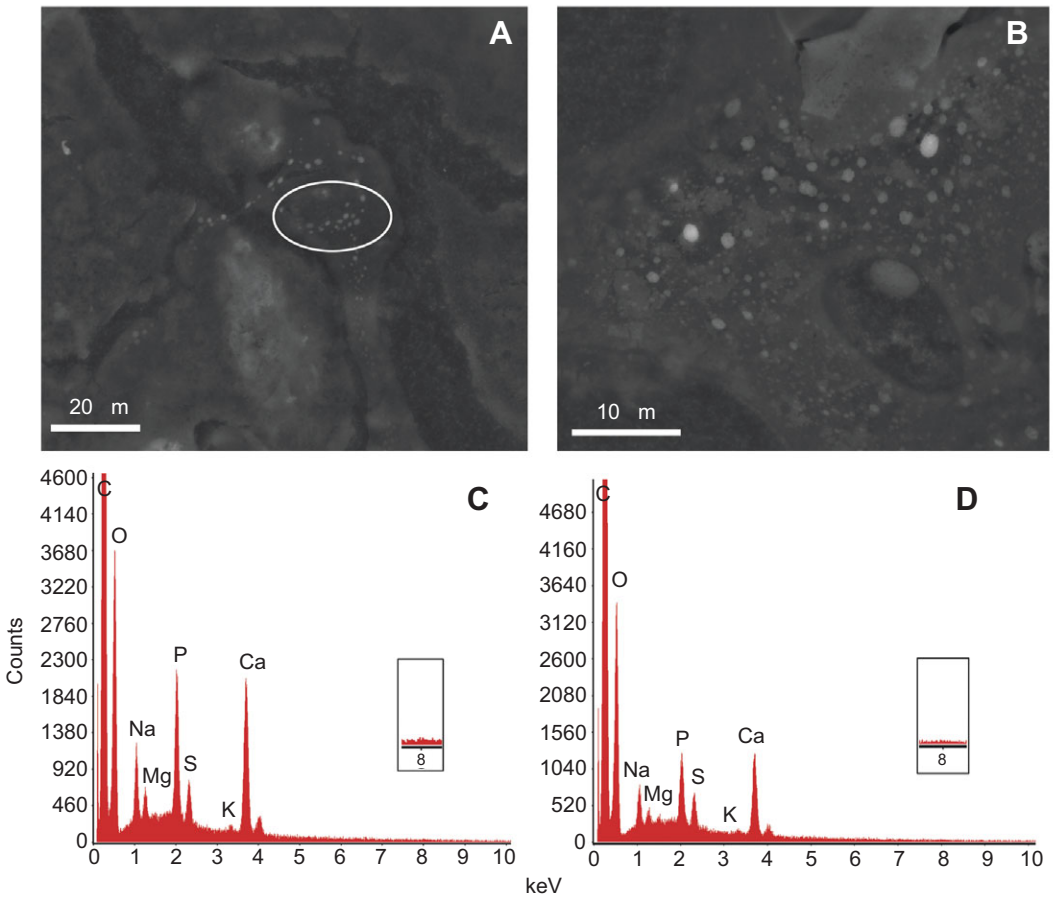

Fig. 6. Granules found in *G. pulex* exposed at Drym for 16 days shown at (A) ×2500 and (B) ×6000 magnification. EDX microanalysis of granules marked 'a' (C) and 'b' (D) show that they are of similar compositions to those of granules in Fig. 4, with Ca, P and O being the most abundant minerals. However, neither Cu nor Zn was detected in granules (magnified inset on the EDX analysis shows no peaks that correspond to Cu at 8 keV, as opposed to granules analysed in Fig. 4).

the granules, and their abundance in those gammarids exposed at both sites, it is conceivable that the granules we detected were formed for molting rather than metal detoxification. MT concentrations are also modulated in the crustacean molt. In the blue crab *Callinectes sapidus*, the levels of naturally occurring Cu-MT and Zn-MT varied with molt stages that were directly related to the metabolic need for hemocyanin (copper-based respiratory pigment) and carbonic anhydrase (zinc containing), which are both relied upon during molting (Engel and Brouwer, 1987; Engel and Brouwer, 2001).

In this scenario, molt cycle granules in the posterior caeca might have been used as available sinks to store excess copper concentrations, but this was not their designated function. Thus, one system (metal detoxification) has impressed upon another (molt cycle). Darlington and Gower (Darlington and Gower, 1990) describe a similar situation in larvae of the trichopteran *Plectrocnemia conspersa* following exposure to copper-rich mine waters in Cornwall. Larvae were collected from a metal-rich site and an uncontaminated tributary. Granules were found in larvae from both sites, but those collected at the metal-rich site contained more copper and sulphur. Granules were located dorsally in the larva, within the Malpighian tubules and the cuticle, which is darker than the ventral side. The primary function of these granules was pigmentation rather than detoxification, but, as

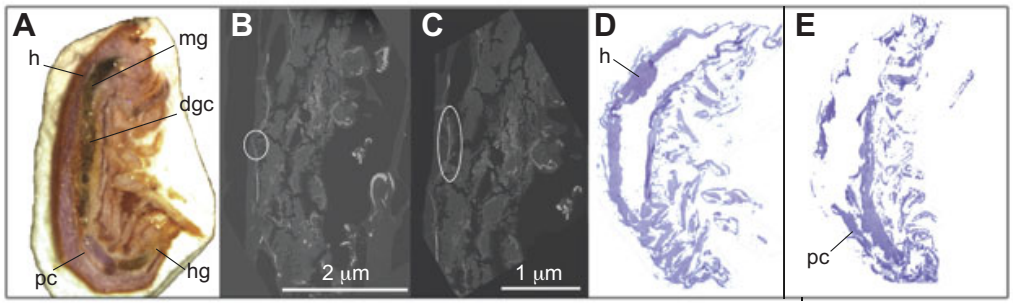

Fig. 7. Location of granules in *G. pulex*. (A) A mounted freeze-dried cross-section illustrating the general anatomy of *G. pulex* with reference to those structures of particular interest (h, heart; mg, midgut; dgc, digestive caeca; pc, posterior caeca; hg, hind gut). Cryostat sections at (B) ×52 and (C) ×100 magnifications show the location of granules (circled) in *G. pulex* exposed at Relubbus for 16 days (Fig. 4). Two stained masses show the position of the (D) heart and (E) the posterior caeca. Granules were located in an area that corresponds to the position of the posterior caeca.

granules contained copper from the pigment, they were available to store excess copper in those larvae collected from the contaminated site. In *Plectrocnemia conspersa*, it was hypothesised that the granules were shed with the old cuticle, thus ridding the organism of excess metal. Darlington and Gower (Darlington and Gower, 1990) showed, as this study also implies, that metals can be stored insolubly in granules that are not specifically synthesised for that function. The exoskeleton molt might be an incidental route for metal elimination in *G. pulex*. The release of metals through ecdysis has been recorded in other crustaceans. In the grass shrimp *Palaemones pugio*, 11%, 18% and 26% of the total body burden copper, zinc and cadmium, respectively, was recovered in the shed exoskeleton (Keteles and Fleegar, 2001). Similarly, in the fiddler crab *Uca pugnax*, molting caused a 12%, 22% and 76% reduction in copper, zinc and lead body burdens in post-moult crabs (Bergey and Weis, 2007).

In this study, we aimed to identify the metal binding properties of two subcellular fractions that are implicated in detoxification in *G. pulex* exposed to accumulated copper and zinc. Metal in the heat-stable cytosol was predominantly associated with a 7.5 kDa MTLP that appeared to be induced over time when the gammarids were exposed to elevated metal concentrations. Insoluble copper was found in calcium-containing granules located to an area analogous to the posterior caeca, rather than the ventral caeca. While ventral caeca granules are often thought to be excreted through the digestive system, granules in the posterior caeca are related to molting. These granules do not preclude the existence of additional copper- or zinc-sequestering granules, or insoluble binding in other parts of the organism, but might point to an incidental method of releasing accumulated copper through ecdysis. As both MT concentrations and granule formation in crustaceans are impacted upon by molting, it is possible that the need for detoxification might have impacted upon existing processes to act as sinks for potentially toxic labile trace metals.

LIST OF ABBREVIATIONS

DM	dry mass
FM	fresh mass
MT	metallothionein
MTLP	metallothionein-like protein
MRG	metal-rich granule
SEM	scanning electron microscope
EDX	energy-dispersive x-ray

ACKNOWLEDGEMENTS

We thank P. S. Rainbow for his comments on draft versions of this manuscript and the valuable guidance of A. J. Morgan (Cardiff University) and T. Brain (King's College London) with sectioning and imaging of *G. pulex* samples. We also thank the anonymous reviewers for their helpful comments.

FUNDING

This research was supported by a PhD research grant from the Natural Environment Research Council [NERC, grant no. NER/S/A2004/1215 to C.H.].

REFERENCES

Adams, S. M., Shorey, C. D. and Byrne, M. (1997). An ultrastructural and microanalytical study of metal-ion content in granular concretions of the freshwater mussel *Hyridella depressa*. *Micron.* **28**, 1-11.

Agrawal, V. P. (1965). Feeding appendages and the digestive system of *Gammarus pulex*. *Acta Zool.* **46**, 67-82.

Al-Mohanna, S. Y. and Nott, J. A. (1987). R-cells and the digestive cycle in *Penaeus semisulcatus* (Crustacea, Decapoda). *Mar. Biol.* **95**, 129-137.

Al-Mohanna, S. Y. and Nott, J. A. (1989). Functional cytology of the hepatopancreas of *Penaeus semisulcatus* (Crustacea, Decapoda) during the molt cycle. *Mar. Biol.* **101**, 535-544.

Barka, S. (2007). Insoluble detoxification of trace metals in a marine copepod *Tigriopus brevicornis* (Muller) exposed to copper, zinc, nickel, cadmium, silver and mercury. *Ecotoxicology* **16**, 491-502.

Bergey, L. L. and Weis, J. S. (2007). Molting as a mechanism of depuration of metals in the fiddler crab, *Uca pugnax*. *Mar. Environ. Res.* **64**, 556-562.

Bradford, M. M. (1976). Rapid and sensitive method for quantitation of microgram quantities of protein utilizing principle of protein–dye binding. *Anal. Biochem.* **72**, 248-254.

Cain, D. J., Luoma, S. N. and Wallace, W. G. (2004).Linking metal bioaccumulation of aquatic insects to their distribution patterns in a mining-impacted river. *Environ. Toxicol. Chem.* **23**, 1463-1473.

Canesi, L., Ciacci, C., Piccoli, G., Stocchi, V., Viarengo, A. and Gallo, G. (1998). *In vitro* and *in vivo* effects of heavy metals on mussel digestive gland hexokinase activity: the role of glutathione. *Comp. Biochem. Physiol. C.* **120**, 261-268.

Cheung, M. S. and Wang, W. X. (2005). Influence of subcellular metal compartmentalization in different prey on the transfer of metals to a predatory gastropod. *Mar. Ecol. Prog. Ser.* **286**, 155-166.

Colvin, R. A., Holmes, W. R., Fontaine, C. P. and Maret, W. (2010). Cytosolic zinc buffering and muffling: Their role in intracellular zinc homeostasis. *Metallomics* **2**, 306-317.

Correia, A. D., Costa, M. H., Ryan, K. P. and Nott, J. A. (2002). Studies on biomarkers of copper exposure and toxicity in the marine amphipod *Gammarus locusta* (Crustacea): I. Copper-containing granules within the midgut gland. *J. Mar. Biol. Assoc. U.K.* **82**, 827-834.

Darlington, S. T. and Gower, A. M. (1990). Location of copper in larvae of *Plectrocnemia conspersa* (Curtis) (Trichoptera) exposed to elevated metal concentrations in a mine drainage stream. *Hydrobiologia* **196**, 91-100.

Elia, A. C., Fanetti, A., Dörr, A. J. M. and Taticchi, M. I. (2008). Effects of concentrated drinking water injection on glutathione and glutathione-dependent enzymes in liver of *Cyprinus carpio* L. *Chemosphere* **72**, 791-796.

Elia, A. C., Dörr, A. J. M., Abete, M. C. and Prearo, M. (2010). Seasonal variability of detoxificant response and heavy metal accumulation in tissues of both sexes in *Tinca tinca* (L.) from Lake Trasimeno. *Rev. Fish. Biol. Fisheries* **20**, 425-434.

Engel, D. W. and Brouwer, M. (1987). Metal regulation and molting in the blue crab, *Callinectes sapidus*-metallothionein function in metal metabolism. *Biol. Bull.* **173**, 239-251.

Engel, D. W., Brouwer, M. and Mercalo-Allen, R. (2001). Effects of molting and environmental factors on trace metal body-burdens and hemocyanin concentrations in the American lobster, *Homarus americanus*. *Mar. Environ. Res.* **52**, 257-269.

George, S. G. (1983). Heavy metal detoxication in the mussel *Mytilus edulis*-composition of Cd-containing kidney granules (tertiary lysosomes). *Comp. Biochem. Physiol. C. Pharmacol. Toxicol. Endocrinol.* **76**, 53-57.

George, S. G., Coombs, T. L. and Pirie, B. J. S. (1982). Characterization of metal-containing granules from the kidney of the common mussel, *Mytilus edulis*. *Biochim. Biophys. Acta* **716**, 61-71.

Graf, F. and Meyran, J. C. (1983). Premolt calcium secretion in midgut posterior ceca of the crustacean *Orchestia*-ultrastructure of the epithelium. *J. Morphol.* **177**, 1-23.

Graf, F. and Meyran, J. C. (1985). Calcium reabsorption in the posterior ceca of the midgut in a terrestrial crustacean, *Orchestia cavimana*-ultrastructural changes in the postexuvial epithelium. *Cell Tissue Res.* **242**, 83-95.

Hamer, D. H. (1986). Metallothionein. *Annu. Rev. Biochem.* **55**, 913-951.

Hennig, H. F.-K. O. (1986). Metal binding proteins as metal pollution indicators. *Environ. Health Perspect.* **65**, 175-187.

Hogstrand, C. and Haux, C. (1991). Binding and detoxification of heavy metals in lower vertebrates with reference to metallothionein. *Comp. Biochem. Physiol. C Toxicol. Pharmacol.* **100**, 137-141.

Hogstrand, C., Verbost, P. M., Bonga, S. E. W. and Wood, C. M. (1996). Mechanisms of zinc uptake in gills of freshwater rainbow trout: Interplay with calcium transport. *Am. J. Physiol. Regul. Integr. Comp. Physiol.* **270**, R1141-R1147.

Hopkin, S. P. (1989). *Ecophysiology of Metals in Terrestrial Invertebrates.* London: Elsevier.

Icely, J. D. and Nott, J. A. (1980). Accumulation of copper within the hepatopancreatic ceca of *Corophium volutator* (Crustacea, Amphipoda). *Mar. Biol.* **57**, 193-199.

Jenny, M. J., Ringwood, A. M., Schey, K., Warr, G. W. and Chapman, R. W. (2004). Diversity of metollothioneins in the American oyster *Crassostrea virginica*, revealed by transcriptomic and proteomic approaches. *Eur. J. Biochem.* **271**, 1702-1712.

Kendrick, M. J., May, M. T., Plishka, M. J. and Robinson, K. D. (1992). *Metals in Biological Systems.* Chichester: Ellis Horwood.

Keteles, K. A. and Fleegar, J. W. (2001). The contribution of ecdysis to the fate of copper, zinc and cadmium in grass shrimp, *Palaemonetes pugio* Holthius. *Mar. Pollut. Bull.* **42**, 1397-1402.

Khan, F. R., Bury, N. R. and Hogstrand, C. (2010a). Cadmium bound to metal rich granules and exoskeleton from *Gammarus pulex* causes increased gut lipid peroxidation in zebrafish following single dietary exposure. *Aquat. Toxicol.* **96**, 124-129.

Khan, F. R., Bury, N. R. and Hogstrand, C. (2010b). Differential uptake and oxidative stress response in zebrafish fed a single dose of the principal copper and zinc enriched sub-cellular fractions of *Gammarus pulex*. *Aquat. Toxicol.* **99**, 466-472.

Khan, F. R., Irving, J. R., Bury, N. R. and Hogstrand, C. (2011). Differential tolerance of two *Gammarus pulex* populations transplanted from different metallogenic regions to a polymetal gradient. *Aquat. Toxicol.* **102**, 95-103.

Kojima, Y. (1991). Definitions and nomenclature of metallothioneins. In *Methods in Enzymology*, Vol. 205, *Metallobiochemistry Part B Metallothionein and Related Molecules* (ed. J. F. Riordan and B. L. Vallee), pp. 8-10. San Diego: Academic Press.

Luoma, S. N. and Rainbow, P. S. (2008). *Metal contamination in aquatic environments: Science and lateral management.* Cambridge: Cambridge University Press.

Maret, W. (2009). Molecular aspects of human cellular zinc homeostasis: redox control of zinc potentials and zinc signals. *Biometals* **22**, 149-157.

Meyran, J. C., Graf, F. and Nicaise, G. (1984). Calcium pathway through a mineralizing epithelium in the crustacean Orchestia in pre-molt: Ultrastructural cytochemistry and x-ray microanalysis. *Tissue Cell* **16**, 269-286.
Meyran, J. C., Graf, F. and Nicaise, G. (1986). Pulse discharge of calcium through a demineralizing epithelium in the crustacean Orchestia: Ultrastructural cytochemistry and x-ray microanalysis. *Tissue Cell* **18**, 267-283.
Morris, C. A., Nicolaus, B., Sampson, V., Harwood, J. L. and Kille, P. (1999). Identification and characterization of recombinant metallothionein protein from a marine alga, *Fucus vesiculosus*. *Biochem. J.* **338**, 553-560.
Mounaji, K., Erraiss, N. E. and Wegnez, M. (2002). Identification of metallothionein in *Pleurodeles waltl. Z. Naturforsch. C* **57**, 727-731.
Mouneyrac, C., Amiard, J. C., Amiard-Triquet, C., Cottier, A., Rainbow, P. S. and Smith, B. D. (2002). Partitioning of accumulated trace metals in the talitrid amphipod crustacean *Orchestia gammarellus*: a cautionary tale on the use of metallothionein-like proteins as biomarkers. *Aquat. Toxicol.* **57**, 225-242.
Nassiri, Y., Rainbow, P. S., Amiard-Triquet, C., Rainglet, F. and Smith, B. D. (2000). Trace-metal detoxification in the ventral caeca of *Orchestia gammarellus* (Crustacea: Amphipoda). *Mar. Biol.* **136**, 477-484.
Ng, T. Y.-T., Rainbow, P. S., Amiard-Triquet, C., Amiard, J. C. and Wang, W. X. (2007). Metallothionein turnover, cytosolic distribution and the uptake of Cd by the green mussel *Perna viridis*. *Aquat. Toxicol.* **84**, 153-161.
Rainbow, P. S. (2007). Trace metal bioaccumulation: Models, metabolic availability and toxicity. *Environ. Int.* **33**, 576-582.
Roesijadi, G. (1996). Metallothionein and its role in toxic metal regulation. *Comp. Biochem. Physiol. C Pharmacol. Toxicol. Endocrinol.* **113**, 117-123.
Scheuhammer, A. M. and Cherian, M. (1991). Quantification of metallothionein by silver saturation. In *Methods in Enzymology*, Vol. 205, *Metallobiochemistry Part B Metallothionein and Related Molecules* (ed. J. F. Riordan and B. L. Vallee), pp. 78-83. San Diego: Academic Press.
Schmitz, E. H. (1992). Amphipoda. In *Microscopic Anatomy of Invertebrates. Vol. 9, Crustacea* (ed. F. W. Harrison and A. G. Humes), pp. 443-528. New York: Wiley-Liss.
Schultz, T. W. (1976). Ultrastructure of hepatopancreatic ceca of *Gammarus minus*. (Crustacea, Amphipoda). *J. Morphol.* **149**, 383-399.
Singhal, R. K., Anderson, M. and Meister, A. (1987). Glutathione, a first line of defense against cadmium toxicity. *FASEB J.* **1**, 220-223.
Vijver, M. G., Van Gestel, C. A. M., Lanno, R. P., Van Straalen, N. M. and Peijnenburg, W. J. G. M. (2004). Internal metal sequestration and its ecotoxicological relevance: A review. *Environ. Sci. Technol.* **38**, 4705-4712.
Wallace, W. G. and Luoma, S. N. (2003). Subcellular compartmentalization of Cd and Zn in two bivalves. II. Significance of trophically available metal (TAM). *Mar. Ecol. Prog. Ser.* **257**, 125-137.
Wallace, W. G., Lee, B. G. and Luoma, S. N. (2003). Subcellular compartmentalization of Cd and Zn in two bivalves. I. Significance of metal-sensitive fractions (MSF) and biologically detoxified metal (BDM). *Mar. Ecol. Prog. Ser.* **249**, 183-197.
Warley, A. (1997). X-ray microanalysis for biologists. In *Practical Methods in Electron Microscopy*, Vol. 16 (ed. A. M. Glauert). Cambridge: Cambridge University Press.
Winge, D. R. (1991). Copper coordination in metallothionein. In *Methods in Enzymology*, Vol. 205, *Metallobiochemistry Part B Metallothionein and Related Molecules* (ed. J. F. Riordan and B. L. Vallee), pp. 458-469. San Diego: Academic Press.
Wu, J. P. and Chen, H. C. (2005). Metallothionein induction and heavy metal accumulation in white shrimp *Litopenaeus vannamei* exposed to cadmium and zinc. *Comp. Biochem. Physiol. C Toxicol. Pharmacol.* **140**, 383-394.